JOURNAL OF AIRCRAFT
Vol. 41, No. 5, September–October 2004

Transient Helicopter Rotor Wakes in Response to Time-Dependent Blade Pitch Inputs

Shreyas Ananthan* and J. Gordon Leishman†
University of Maryland, College Park, Maryland 20742

A time-accurate, free-vortex method was used to predict the evolution of a helicopter rotor wake and the corresponding unsteady rotor airloads in response to time-varying changes in blade pitch. Both steady and maneuvering flight conditions were examined. The modeling was validated using measured rotor responses to transient increases in collective pitch and also for oscillatory collective and cyclic blade pitch inputs. In each case the results showed that there was a temporal lag in the growth and convection of vorticity into the rotor wake, causing significant unsteady effects at the rotor. For transient blade pitch inputs the calculated results showed the bundling of individual vortex filaments below the rotor into vortex rings, a result also verified experimentally. These vortex rings, however, subsequently break down through the development of Kelvin waves. A simulated piloted pull-up maneuver from descending flight was studied, producing evidence that maneuvers can also cause wake vorticity to bundle below the rotor. Large unsteady rotor airloads were produced as the blades encountered this accumulated wake vorticity. A study was also conducted to examine the effects of small-amplitude, low-frequency blade pitch inputs, typical of pilot control inputs during flight. Overall, it is apparent that even moderate control inputs can have a significant impact on the temporal developments of the rotor wake.

Nomenclature

A	=	rotor disk area, πR^2, m^2
C_T	=	rotor thrust coefficient, $T/(\rho A \Omega^2 R^2)$
c	=	rotor blade chord, m
N_b	=	number of blades
p	=	roll rate, rad s^{-1}
q	=	pitch rate, rad s^{-1}
R	=	rotor radius, m
r	=	yaw rate, rad s^{-1}
r	=	radial distance, m
$\boldsymbol{r}$	=	position vector of a wake marker, m
r_c	=	viscous core radius, m
r_0	=	initial core radius, m
T	=	rotor thrust, N
t	=	time, s
$\boldsymbol{V}$	=	velocity vector at a wake marker, ms^{-1}
$\boldsymbol{V}_{\text{ex}}$	=	external velocity field, ms^{-1}
$\boldsymbol{V}_{\text{ind}}$	=	induced velocity, ms^{-1}
$\boldsymbol{V}_\infty$	=	freestream velocity, ms^{-1}
v_h	=	hover-induced velocity, ms^{-1}
x, y, z	=	Cartesian coordinate system, m, m, m
α	=	Lamb–Oseen constant = 1.25643
β	=	blade–flapping angle, rad
Γ_v	=	tip vortex strength (circulation), m^{2}s^{-1}
δ	=	effective (turbulent) eddy viscosity coefficient
ε	=	filament strain
ζ	=	wake (vortex) age, rad
ζ_0	=	effective origin offset, rad
λ	=	nondimensional velocity, $v/\Omega R$
λ_a	=	nondimensional inflow amplitude
λ_h	=	nondimensional induced velocity in hover, $\sqrt{(C_T/2)}$
μ	=	advance ratio, $V_\infty/\Omega R$
ν	=	kinematic viscosity, m^{2}s^{-1}
ρ	=	flow density, kg m^{-3}
σ	=	rotor solidity, $N_b c/\pi R$
ψ	=	azimuth angle, rad
ψ_b	=	reference blade azimuthal location, rad
Ω	=	rotor rotational speed, rad s^{-1}
$\boldsymbol{\omega}$	=	vorticity, m^{2}s^{-1}

Received 3 July 2003; revision received 16 September 2003; accepted for publication 17 September 2003.

*Graduate Research Assistant, Department of Aerospace Engineering, Glenn L. Martin Institute of Technology, Alfred Gessow Rotorcraft Center; shreyas@glue.umd.edu.

†Professor, Department of Aerospace Engineering, Glenn L. Martin Institute of Technology, Alfred Gessow Rotorcraft Center; leishman@eng.umd.edu.

Introduction

THE better modeling of the unsteady, aperiodic nature of helicopter rotor aerodynamics is important for understanding and predicting many challenging problems associated with helicopter flight.[1] It is the behavior of helicopters undergoing transient, maneuvering flight that is of particular interest to the analyst. This is because maneuvering often sets the limits to overall flight capabilities of helicopters. The rotor airloads, acoustics, and overall helicopter handling qualities in maneuvers are yet to be predicted with sufficient accuracy, in part because of the difficulties in predicting the physical nature of the time-dependent developments of the rotor wake. This is particularly important during descending flight or any other flight conditions where the rotor might come close to or ingest part of its own vortical wake. The resulting blade-wake and blade-vortex interactions (BVIs) are a source of large unsteady aerodynamics loads and rotor noise.[2] The stringent noise regulations enforced nowadays mean that a thorough understanding and prediction capability for the rotor wake is clearly essential.

The vortical nature of a helicopter rotor flowfield is dominated by discrete vortices, which trail from the tips of each blade.[3] Other vortical wake structures such as the inner wake sheet from the blade play a role in determining the overall wake evolution,[4] but the tip vortices are of principal importance. At a minimum, therefore, the key to predicting the performance and airloads acting on the helicopter is to determine the strengths, locations, and net velocity field induced by the tip vortices as they are convected inside the rotor wake. In many cases these tip vortices linger near the rotor, and so their structure must be modeled accurately until they are several revolutions old. This is a formidable problem and can only be solved subject to various levels of physical and numerical approximation.

A further complication is that the aerodynamic response at the rotor to changes in flight condition is not instantaneous and takes place over a significant time in terms of rotor revolutions. As with

many unsteady aerodynamic phenomena, the timescales of rotor flow adjustments can be surprisingly long. Rotor-wake predictions then can be very different compared to what might be obtained by invoking periodic flow assumptions, a common assumption used in many wake analyses (see Ref. 5). In some types of maneuvers, the timescales associated with the wake developments can be close to the duration of the maneuver itself, for example, during sharp pull-ups, wind-up turns, roll reversals, etc. Under these conditions, accurate modeling of the time dependence of the wake becomes much more important. Furthermore, during maneuvers the tip vortices can also convect much closer to the blades and to each other, making the detailed modeling of vortex–surface and vortex–vortex interactions critical.

Recent literature[6–8] has amply stressed the need for improved time-accurate rotor-wake models for better rotor airloads and helicopter aeromechanics predictions. Experience suggests that the dynamic evolution of the rotor wake can be better predicted in some maneuvering conditions than in others. It has been suggested that significant differences between flight mechanics simulations and observations can be traced to inaccurate, or incomplete, modeling of the temporal development of the rotor wake. This is especially the case for the problematic off-axis response of the helicopter to pilot control inputs in maneuvering flight.[6] For steady rolls with small imposed angular rates, the effects can be predicted to some level of accuracy with linearized dynamic inflow models (e.g., Ref. 9) or with other forms of "prescribed" wake models (e.g., Refs. 10 and 11). In either case an underlying assumption is that the rotor wake retains its mostly regular helicoidal form and is distorted during maneuvering flight according to prescribed rules. However, such linearized models do not provide sufficiently good descriptions of the rotor aerodynamics under transient, maneuvering flight conditions. This is not only because the wake development is aperiodic in time, but the problem becomes highly nonlinear, especially if the regular helicoidal form of the wake breaks down causing flow recirculation. This means that the computation of rotor aerodynamics and the rotor-wake evolution must be approached at more rigorous level of approximation, despite the penalty of much greater modeling complexity and correspondingly higher computational costs.

The physics of transient rotor-wake behavior can be seen in the early work of Taylor,[12] who conducted a series of wake flow visualizations for an impulsively started rotor. It was observed that the wake vortices initially tended to bundle together below the rotor, forming a toroidal "ring" of accumulated vorticity. This ring can be viewed as the analogy to the well-known starting vortex observed from airfoils in response to rapid changes in angle of attack, which is an artifact of Kelvin's theorem.[13] Although Taylor performed only flow visualization, it was further shown by Carpenter and Friedovich[14] that rapid control inputs can appreciably affect the rotor inflow and rotor airloads in the initial stages after the control inputs. More recently, flow-visualization results documenting the wake structure in response to transient blade pitch inputs have been obtained by Jessurun et al.[15]

Although rapid, large-amplitude control inputs and their effects on the wake are of much value in understanding the gross feature of the wake evolution, in most practical cases control inputs are smaller in amplitude and are applied at low frequency. Under these conditions the aerodynamic effects take place on somewhat smaller flow scales, so that predicting accurately the details of the resulting wake developments is important if the effects on the rotor are to be evaluated properly. Unsteady effects introduced by time-varying pilot control inputs will affect the blade loads, which then affect the tip vortex strengths and their detailed interactions, and so affect the resulting wake evolution. In some cases the effects of control inputs can be quite subtle, but can have pronounced nonlinear effects on the resulting aerodynamic response of the rotor. The dynamic response of the rotor wake to pilot control inputs at low and intermediate frequencies below the rotational frequency is of particular interest from the perspective of helicopter flight dynamics and aircraft handling qualities. The aerodynamic problem is compounded again, however, when aperiodic pilot control inputs are applied during maneuvering flight conditions, making both the understanding and prediction of the time-dependent rotor aerodynamics extremely complex.

The objective of the present paper is threefold. The first part is to demonstrate the applicability and numerical robustness of a recently developed time-accurate free-vortex wake model in computing the rotor aerodynamic response to time-dependent control inputs. The high computational costs and numerical limitations encountered with several other types of methods in preserving concentrated rotor wake vorticity[16] otherwise severely limit the ability to analyze these types of very practical problems. The vortex wake model uses the time-accurate scheme of Bhagwat and Leishman,[5,17,18] which has recently been extended by Ananthan et al.[19] to include the modeling of filament strain and viscous diffusion effects using a viscous splitting approach. The second part is to further understand the physics of the rotor wake structure in response to blade control inputs. It is shown that the often observed time lags in the aerodynamic response of the rotor to blade pitch inputs is a consequence of temporal developments in the dynamic wake structure, which involves the accumulation and tight bundling of vorticity below the rotor. Comparisons of the computed aerodynamic responses with experimental data and flow visualizations are made, where available. The third part to highlight the enormous aerodynamic complexity of the rotor wake during transient maneuvering problems and to show that the understanding and modeling of the rotor wake and rotor response under these conditions is far from being complete.

Methodology

Free-Vortex Wake Scheme

The rotor aerodynamics model is based on a time-accurate free-vortex wake method.[5] This method is based on the assumption of an incompressible flow, with all of the vorticity in the rotor wake being assumed concentrated within discrete vortex filaments. A description of the vorticity field in the rotor wake is governed by the three-dimensional, incompressible Navier–Stokes equations, which in a Lagrangian form can be written as

$$\frac{\mathrm{D}\boldsymbol{\omega}}{\mathrm{D}t} = \underbrace{(\boldsymbol{\omega}\cdot\nabla)\boldsymbol{V}}_{\text{strain}} + \underbrace{\nu\Delta\cdot\boldsymbol{\omega}}_{\text{diffusion}} \tag{1}$$

This equation defines the change of vorticity of a fluid element moving with the flow in terms of the instantaneous value of vorticity $\boldsymbol{\omega}$ and the local velocity field $\boldsymbol{V}$. The term on the left-hand side of Eq. (1) represents advection (convection), with the two terms on the right-hand side being a strain or "stretching" term and viscous diffusion term, respectively. In many practical problems, it can be justified that viscous phenomena will be confined to much smaller length scales compared to potential flow phenomena. Therefore, vortex methods use discrete line vortices to represent concentrated lines of vorticity. Under these conditions, Helmholtz's second law states that the vortex lines move freely as material lines.[13] In this case, Eq. (1) reduces to a simpler equation of the form

$$\frac{\mathrm{d}}{\mathrm{d}t}\boldsymbol{r} = \boldsymbol{V}, \qquad \boldsymbol{r}(t=0) = \boldsymbol{r}_0 \tag{2}$$

where $\boldsymbol{r}_0$ is some initial position vector of the marker and $\boldsymbol{V}$ is the local velocity at that marker. In the present model each filament is defined by the position of two adjacent contiguous Lagrangian markers (see Fig. 1), and Eq. (2) applies to the behavior of each and every marker. Notice that the right-hand side of Eq. (2) is a highly nonlinear term resulting from the self- and mutually induced velocities of the entire rotor and its wake structure. It is computed (at some considerable numerical expense) using the repeated application of the Biot–Savart law to the discretized vorticity field. The wake field is comprised of vortices with finite viscous cores of radius r_c (see later).

The position vector $\boldsymbol{r}$ of a Lagrangian marker is a function of both the age of the vortex filament ζ and the time (or blade azimuth angle) at which the filament was trailed into the rotor wake ψ. The governing equation for the free movement of the vortices in the

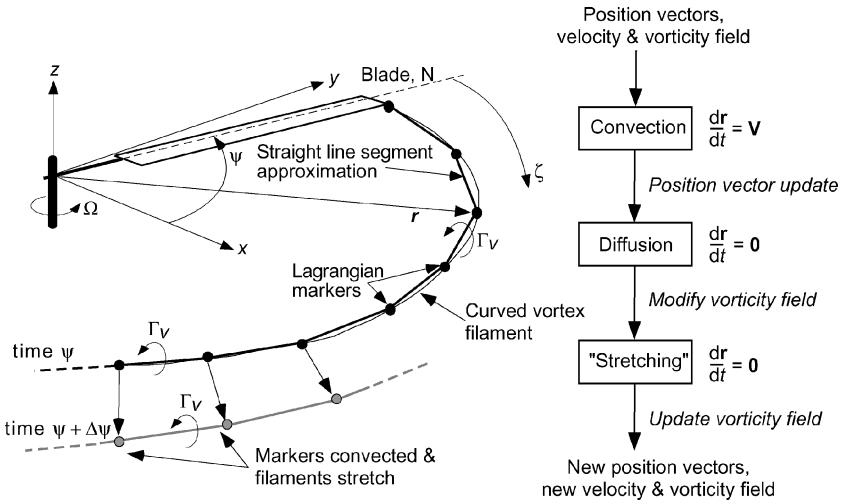

Fig. 1 Schematic showing free-vortex wake scheme.

rotor wake, therefore, becomes a partial differential equation of the form

$$\frac{\partial \boldsymbol{r}(\psi,\zeta)}{\partial \psi} + \frac{\partial \boldsymbol{r}(\psi,\zeta)}{\partial \zeta} = \frac{1}{\Omega}\boldsymbol{V}[\boldsymbol{r}(\psi,\zeta,r_c)] \tag{3}$$

The right-hand side of this equation can be written as

$$\boldsymbol{V} = \boldsymbol{V}_{\text{ind}} + \boldsymbol{V}_{\text{ex}} + \boldsymbol{V}_{\infty} \tag{4}$$

where $\boldsymbol{V}_{\text{ind}} = \boldsymbol{V}_{\text{ind}}(\psi,\zeta,r_c)$ is the induced velocity field from the rotor and all of the vortical elements in the wake, $\boldsymbol{V}_{\text{ex}}$ is an external velocity field such as might be induced by a maneuver, and $\boldsymbol{V}_{\infty}$ is the freestream velocity vector. Equation (3) is solved by the application of finite differences to approximate the space and time derivatives.[5] The displacements of the markers are then found in a time-accurate manner by numerical integration of the governing equations. The present approach uses the second-order-accurate, predictor-corrector scheme (PC2B scheme)[5,18] developed by Leishman et al. and Bhagwat and Leishman.

Viscous and Straining Effects

The additional effects of filament strain and viscous diffusion of the vortex filaments that are convected in the flow are accounted for using a viscous splitting approach.[19] Viscous effects associated with wake vortices are usually confined to much smaller length scales compared to the scale associated with development of the wake. However, under some rotor flight conditions, especially for transient control inputs and during maneuvers, the preponderance of interactions between blades and wake vortex filaments means that the modeling of viscous effects and the velocity field near the filament core must be considered accurately if quantitative predictions are a goal.

Viscous Diffusion Model

The viscous structure and associated diffusion of the vortical filaments can be incorporated using semi-empirical models. Certain algebraic models show good comparisons with the observed swirl and axial velocities measured in rotor tip vortices over a range of relevant wake ages.[20] In the present formulation, the viscous spin down and core growth of the vortex filaments with time is modeled using Bhagwat and Leishman's development of Squire's model.[20] The viscous core radius of a filament relative to the time at which it originated in the flow is given by

$$r_c(\zeta) = \sqrt{4\alpha\delta\nu\left(\frac{\zeta-\zeta_0}{\Omega}\right)} \equiv \sqrt{r_0^2 + \frac{4\alpha\delta\nu\zeta}{\Omega}} \tag{5}$$

where ζ_0 can be viewed as a virtual origin, that is, the vortex filament forms with some initial nonzero viscous core r_0, a fact observed experimentally. The coefficients of this model ζ_0 and δ are defined empirically. The apparent or eddy viscosity δ is a function of the vortex Reynolds number Γ_v/ν (see Refs. 20 and 21).

Straining Model

Because the Lagrangian markers are allowed to freely convect in the wake solution, the vortex filaments will be strained as adjacent markers move relative to each other. Helmholtz's third law requires the net strength of any vortex filament to remain constant, so that the product of the vorticity and the cross-sectional area over which vorticity is distributed must also remain constant. Stretching the vortex filament, therefore, increases its vorticity and decreases its core size, leading to an increase in the induced velocity surrounding the vortex core. The converse happens when vortices are squeezed. Such straining effects can, therefore, have a significant impact on the wake developments in regions where filaments come into proximity with each other.

Ananthan et al.[19] have shown that in a free-vortex scheme the stretching of the filament can be determined in terms of the velocities of adjacent Lagrangian markers. The vortex filament method requires only the change in the magnitude of the vorticity of each straight filament and not the local vorticity for each fluid particle. Using the conservation laws with the assumption of incompressible flow allows the change in the viscous core radius over which most of the vorticity is distributed to be established using

$$\Delta r_c = r_c\left[1 - (\varepsilon+1)^{-\frac{1}{2}}\right] \tag{6}$$

When combined with viscous diffusion, the net equation governing the development of the vortex core becomes

$$r_c(\zeta,\varepsilon) = \sqrt{r_0^2 + \frac{4\alpha\delta\nu}{\Omega}\int_{\zeta_0}^{\zeta}(1+\varepsilon)^{-1}\,\mathrm{d}\zeta} \tag{7}$$

which is used in the velocity field model on the right-hand side of Eq. (3).

Blade Aerodynamics Model

The rotor was modeled as N_b rigid, articulated blades of finite mass that execute independent, time-dependent flapping motion. Aerodynamically, each blade was modeled using a Weissinger-L type of lifting-surface model. The strength of the concentrated free tip vortex trailed into the rotor wake was determined by assuming that the vorticity outboard of the maximum bound vorticity over the blade span rolls up into the tip vortex. The spanwise tip vortex release

point was determined based on a variation of Rossow's centroid of vorticity approach,[22] which couples the near wake and the far wake to the blade solution through an induced angle of attack at each blade control point. Specifying the vortex release point also satisfies the initial condition requirement in Eq. (2). After the blade lift has been determined consistently with the rotor-wake solution, the aerodynamic flapping moments and rotor forces and moments were directly calculated by integrating the segment loads over the blade span and around the rotor azimuth.

Coupling with Blade Motion

The rotor-wake solution in maneuvering flight or other nonsteady flight condition is closely coupled with the blade-flapping response. Therefore, the individual blade-flapping dynamics must be solved simultaneously with the rotor-wake aerodynamics and to a consistent level of numerical accuracy. The equation of motion of a flapping blade is given by the equilibrium of moments about the flapping hinge (see Ref. 23 for derivations). Because the elemental lift depends on the local induced inflow velocity, the blade-flapping response is dictated by the vortical wake solution. Also, because of the blade attachment boundary condition required for the vortex filaments the wake solution itself depends on the blade-flapping solution. The blade-flapping behavior can be reduced to a set of first-order equations of the form

$$[\dot{\beta}^{\star}] = [F(\beta(\psi), \psi)] \tag{8}$$

where the $\star$ denotes differentiation with respect to ψ. Because the equations governing the rotor wake are also written in the same mathematical form as Eq. (8), they can all be solved simultaneously using the same time-integration algorithm and to a consistent level of numerical approximation.

Results and Discussion

The unsteady wake aerodynamics have been analyzed in response to the forced excitation of collective and cyclic pitch control inputs as a function of time. Both transient (ramp) as well as oscillatory blade pitch inputs (cyclic and collective) have been considered. The tendency of the wake vorticity below the rotor to merge or bundle and produce a form of toroidal ring was one common feature noted in many of the calculations. This wake behavior was found in response to control inputs in steady flight (especially using collective pitch), but also under some maneuvering flight conditions, especially in descending flight where the vortex filaments are generally closer together to begin with. The dynamic accumulation of wake vorticity affects both the timescales of the resulting wake developments, as well as the unsteady airloads produced on the blades. Some experimental data for helicopter rotors operating in hovering flight are available for these conditions, and this provides a good baseline for comparison with the modeling to determine both the accuracy and adequacy of the unsteady airloads and wake predictions. Later, rotor maneuvers will be discussed using simulated pilot control inputs.

Experiments

A literature search uncovered only three experiments that have visualized the wake evolution of a helicopter rotor under transient operating conditions. In all cases, a common feature in the experiments was that the tip vortices pair off in the wake below the rotor and initially form into coherent bundles of almost toroidal rings of concentrated vorticity. These vortex rings are present in the rotor wake for several subsequent rotor revolutions and can have a substantial effect on the overall time history of the resulting wake developments, the developing inflow, and on the blade airloads.

The first experimental study was made by Taylor,[12] who conducted a series of wake flow visualizations for cases when the helicopter rotor was impulsively started with a fixed collective pitch. The balsa dust technique was used to seed the flow, which was illuminated by a light sheet. Figure 2 gives two snapshots of the wake structure reproduced from the work of Taylor,[12] which shows a plane in the wake shortly after the rotor was started. These images

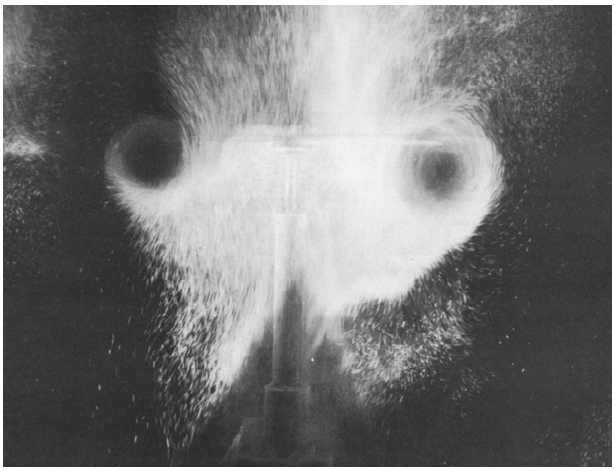

a) Early time

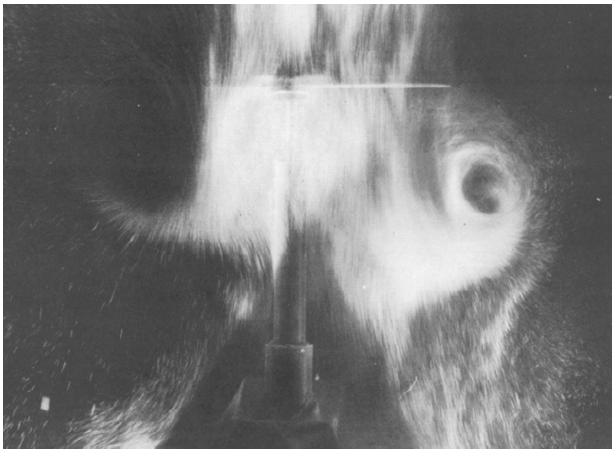

b) Later time

Fig. 2 Flow-visualization image in a vertical plane through the rotor axis documenting the formation of a vortex ring in the wake below an impulsively started hovering rotor: a) early time just after impulsive start and vortex ring development and b) later time, where the ring convects below the rotor. (Photos reproduced from Taylor; Ref. 12.)

are two of the clearest that can be adequately reproduced and show qualitatively the physical nature of the developing rotor wake with good evidence of the starting vortex ring.

Taylor[12] noted that his results were similar to those reported by Carpenter and Friedovich[14] for rapid changes in collective pitch (see next). In this latter test, smoke streamers were used to seed the flow. More recently, similar results have been documented by Jessurun et al.,[15] again by using smoke as the seeding medium. In this experiment, the effects of both rapid collective and cyclic pitch inputs on the resulting wake evolution were examined. It was also seen from the various flow-visualization studies that these starting rings of vorticity begin to break down as they are convected farther away from the rotor. This suggests that the accurate modeling of close vortex filament interactions as well as the time accuracy of the problem will be critical in establishing good predictions of the overall rotor airloads under transient conditions.

Ramp Changes in Collective Pitch

Simulations of the experiments of Carpenter and Friedovich[14] were considered in some detail. In this experiment, the time-dependent rotor response was studied subject to a rapid ramp increase in collective pitch. The three-bladed rotor had a radius of 5.8 m (19 ft) with solidity of 0.042. The rotor was operated at approximately 220 rpm (23.04 rad s^{-1} or 3.67 Hz). The rotor collective pitch was increased linearly from zero at constant rates of 6, 20, 48, and 200 deg per second to a maximum pitch angle of

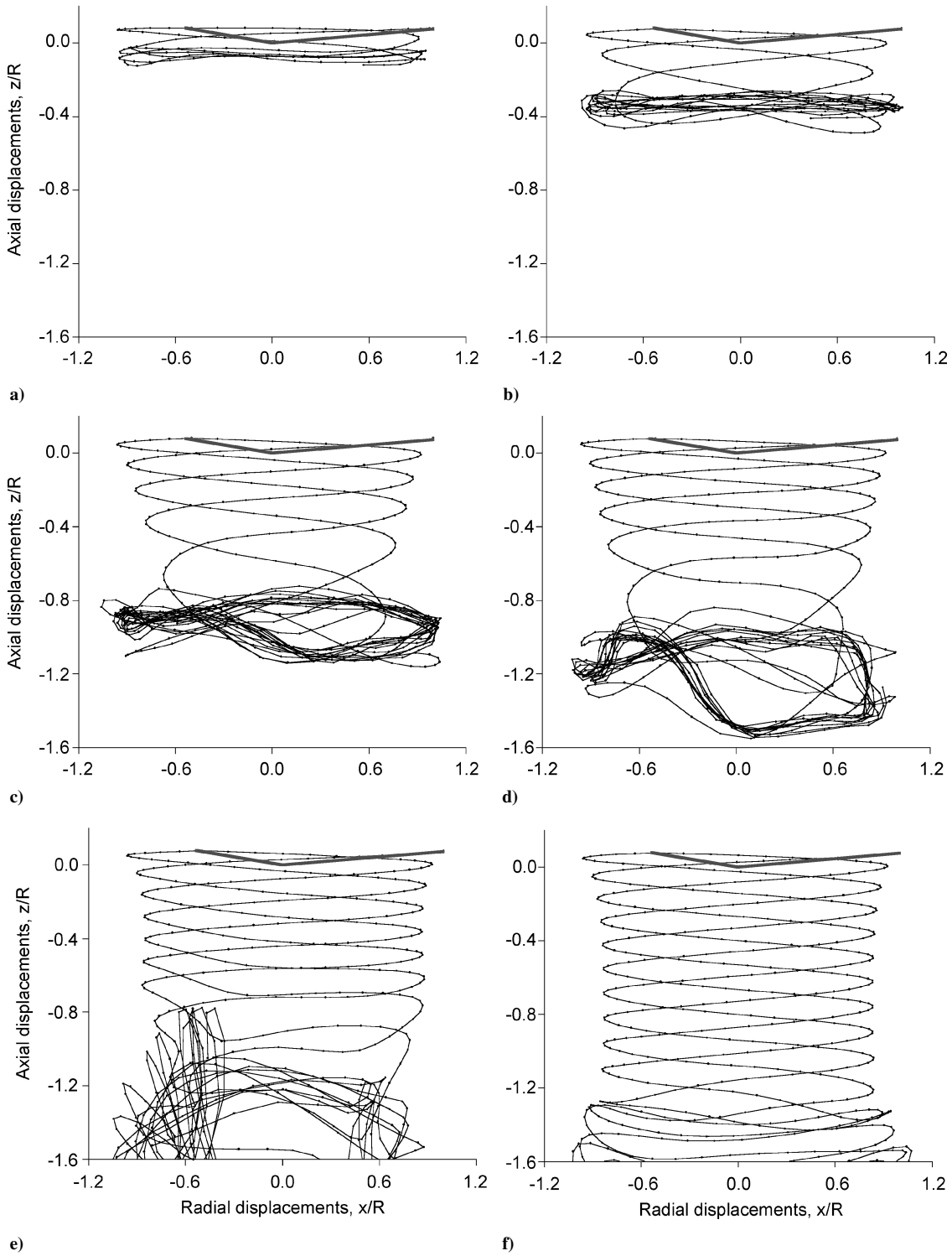

Fig. 3 Free-vortex wake evolution for a hovering rotor undergoing a ramp change in collective pitch at 20 deg/s: a) ψ_b = 1080 deg, b) ψ_b = 1800 deg, c) ψ_b = 2880 deg, d) ψ_b = 3240 deg, e) ψ_b = 3960 deg, and f) ψ_b = 5400 deg.

12 deg. In the experiments, the blade flap angles, the rotor thrust, and the mean rotor inflow were measured as functions of time. Flow visualization was also performed in this experiment, complementing a valuable set of measurements for a relatively simple set of time-dependent blade pitch inputs.

Rotor-Wake Dynamics

The computed evolution of the vortical wake structure is shown in the sequences in Figs. 3–5 for three collective ramp rates of 20, 48, and 200 deg per second, respectively. The geometry of the tip vortices trailing from the three blades is shown at selected times after the collective pitch input was applied. It is apparent that in each case the trailed vortices initially pair off and bundle up below the rotor to form a vortex ring. This is also shown by the flow-visualization images in Fig. 6, which have been reproduced from Carpenter and Friedovich's paper.[14]

Immediately after the collective pitch input was applied, the vortices trailed from the blade tips can only convect relatively slowly away from the rotor because of the initially low thrust and low induced inflow. In fact, by comparing the helicoidal pitch of the computed wake at early times vs later times in each case it is apparent that net inflow through the rotor builds up only relatively slowly

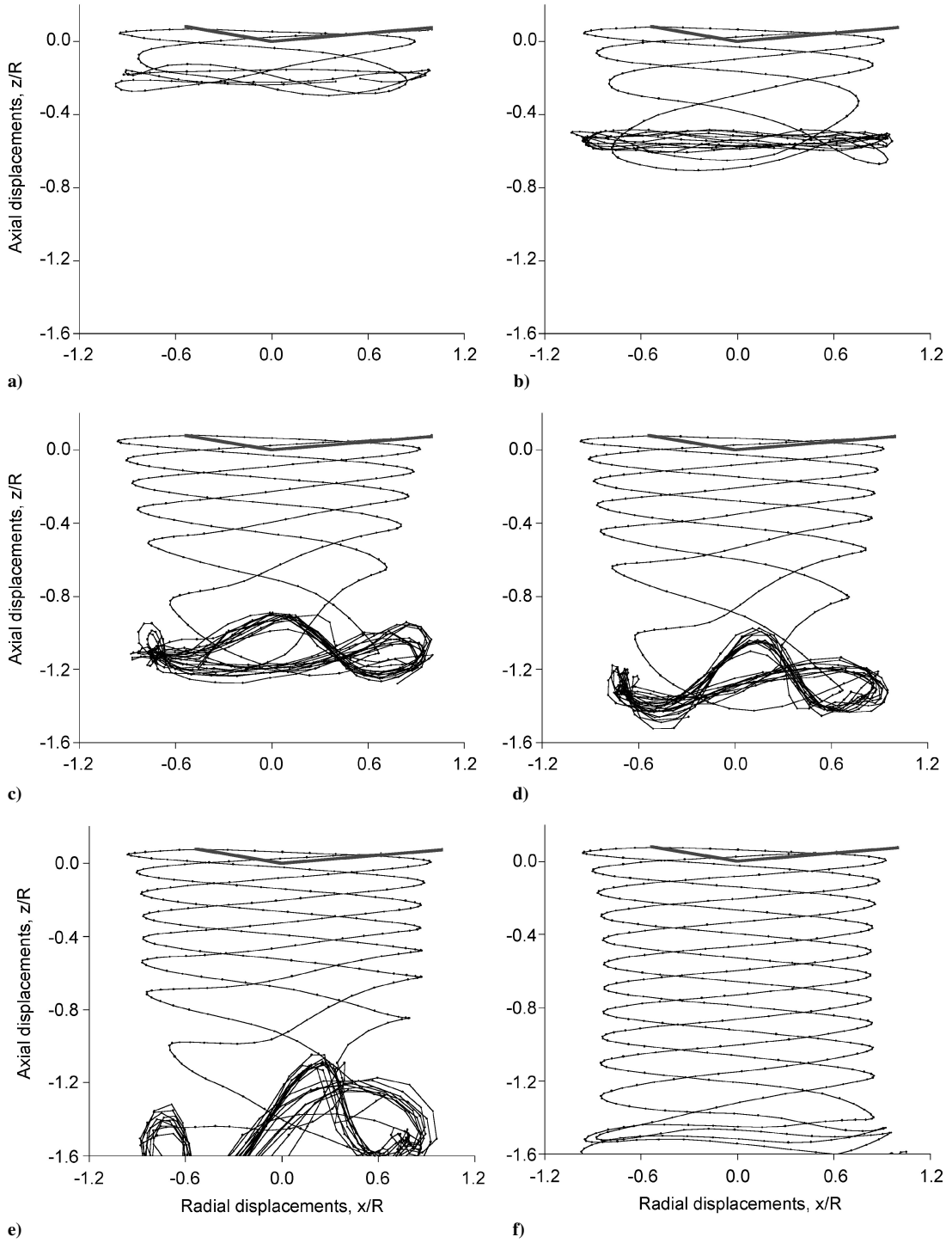

Fig. 4 Free-vortex wake evolution for a hovering rotor undergoing a ramp change in collective pitch at 48 deg/s: a) ψ_b = 1080 deg, b) ψ_b = 1800 deg, c) ψ_b = 2640 deg, d) ψ_b = 2880 deg, e) ψ_b = 3240 deg, and f) ψ_b = 5040 deg.

over several rotor revolutions. Initially, therefore, the tip vortices initially lie in close proximity to each other, and their respective induced velocities create a tendency for them to pair about each other. This is evident in both the calculations shown in Figs. 3–5 and the flow-visualization results in Fig. 6. This pairing tendency is the main reason for the formation of a ring of bundled vorticity immediately below the rotor plane. As previously alluded to, this vortex ring is analogous to a starting vortex system for a wing undergoing a sudden change in angle of attack.

After the wake begins to develop and the inflow through the rotor increases, the newer trailed vortices begin to convect in a relatively higher wake velocity, and the starting ring is convected further down in the wake below the rotor. Notice that in each case the starting vortex structure is unstable and begins to show the presence of pronounced sinusoidal deformation modes or Kelvin waves.[24] These waves grow in amplitude with time and eventually cause the starting vortex system to break down as it convects into the far wake below the rotor.

As the rotor-induced inflow approaches a steady-state value, the vorticity associated with the vortex ring has now been convected downstream well away from the rotor blades. After about four–six rotor revolutions (depending on collective ramp rate), this starting wake has been convected about-one and a-half rotor radii below the rotor. At this point, any instabilities have been convected sufficiently

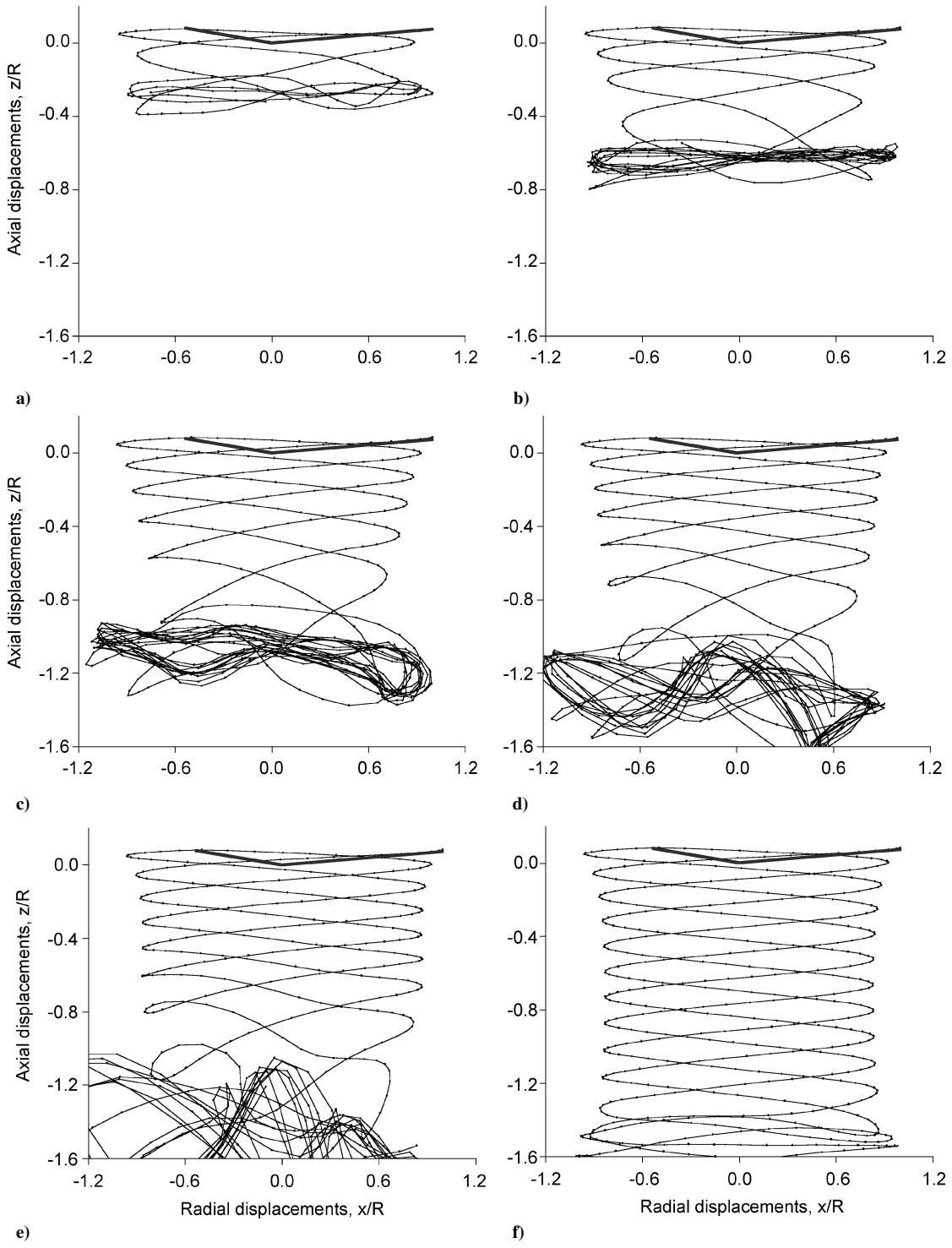

Fig. 5 Free-vortex wake evolution for a hovering rotor undergoing a ramp change in collective pitch at 200 deg/s: a) ψ_b = 1080 deg, b) ψ_b = 1800 deg, c) ψ_b = 2640 deg, d) ψ_b = 3000 deg, e) ψ_b = 3360 deg, and f) ψ_b = 5040 deg.

far away so that their influence on the rotor aerodynamics becomes small. The wake then approaches a steady-state (periodic) condition with the vortex wake structure taking on a more characteristic helicoidal form.

Rotor Thrust and Blade Flapping

Figure 7 gives the predicted results of the thrust and blade flapping, respectively, for three collective pitch rates of 20, 48, and 200 deg per second along with Carpenter and Friedovich's measurements. In each case, the predicted time history of the rotor thrust response and buildup in the blade flapping show good agreement with the experimental measurements. Notice that there is a lag in the development of the rotor thrust, which builds up and reaches its final value in about two–four rotor revolutions, depending on the collective pitch input rate. The intermediate values of the thrust show significant overshoots before settling down to their final values. For the highest ramp rate of 200 deg/s, the thrust overshoot is about twice the steady-state value, confirming the significant effects of transient blade pitch inputs on the overall rotor-wake evolution, blade airloads, and rotor flapping response.

The lag in the mean rotor inflow and thrust overshoots in these experiments was attributed by Carpenter and Friedovich[14] to flow

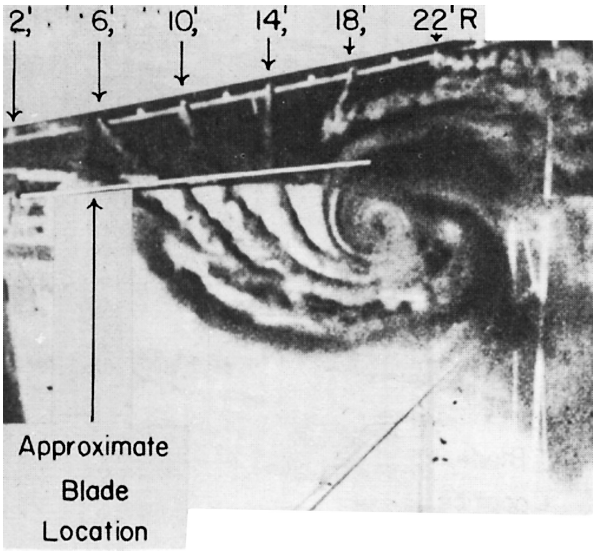

a) Early time

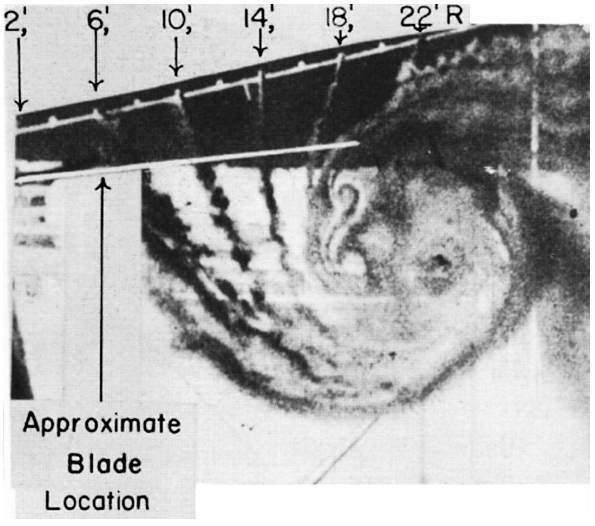

b) Later time

Fig. 6 Flow-visualization images in a vertical plane through the rotor axis showing that pairing of individual tip vortices gives rise to the starting vortex ring. (Photos reproduced from Carpenter and Friedovich; Ref. 14).

inertia effects, that is, a noncirculatory or apparent mass effect. To model this behavior, they obtained a dynamic inflow equation by equating rotor thrust obtained from combined blade element momentum theory (see Ref. 14). In view of the present results, however, it can be concluded that the problem is dominated by the temporal evolution of the vorticity trailed into the rotor wake, that is, it is predominantly a circulatory effect.

Oscillatory Pitch Inputs

The dynamic response of the rotor wake to a step or ramp change in the collective pitch can be idealized by a combination of responses to a series of inputs at several different frequencies. In this section, the behavior of the inflow induced by the rotor wake to oscillatory blade pitch excitation is examined. This problem has been studied experimentally to provide validation of various dynamic inflow models.[25–27] The rotor-wake dynamic response at low and intermediate range of frequencies below the rotational frequency is of particular interest from the perspective of helicopter flight dynamics and handling qualities. This is also important for rotor acoustics, the resulting wake evolution, and changes in the tip vortex positions being closely correlated with rotor noise fluctuations.

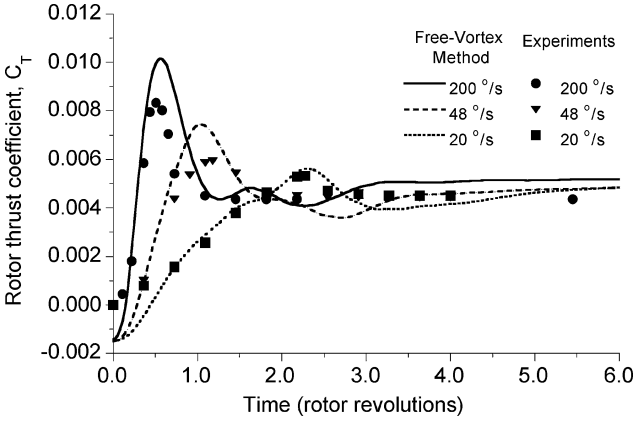

a) Rotor thrust

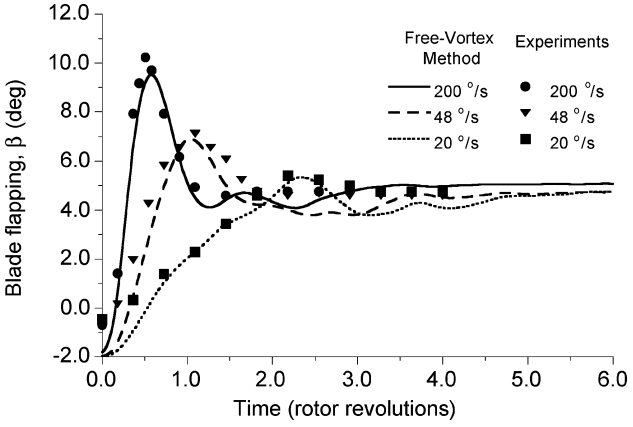

b) Blade flapping

Fig. 7 Time-varying rotor thrust and blade flapping for a ramp change in collective pitch at 20, 48, and 200 deg/s: a) Rotor thrust and b) blade flapping. (Experimental measurements from Carpenter and Friedovich.[14])

Ellenrieder and Brinson[27] have conducted a series of experiments to measure the time-dependent inflow of a hovering rotor in response to sinusoidal excitations of the collective and cyclic pitch. The experiments used a four-bladed model rotor with rectangular blades, which were torsionally soft. Under normal operating conditions these blades had an elastic twist of approximately −6 deg (information provided by Ellenrieder and not documented in Ref. 27). The rotor radius was 0.77 m, the blade chord was 0.06 m, and the rotor was operated at a nominal rotational speed of 1200 rpm (125.66 rad s^{-1} or 20 Hz). The rotor thrust coefficient C_T was 0.013, although the thrust was not measured directly and only estimated. The blade pitch inputs for both collective and cyclic excitations consisted of changes of 1.5 deg in magnitude. The measurement of the inflow velocities was made using hot-wire anemometers at 10 stations along the radius and $0.2R$ below the rotor. A Fourier frequency analysis was used to find the amplitude and phase of the spatial and temporal inflow response, although results for only the first harmonic have been made available.

Collective Pitch Excitation

Collective pitch excitation was accomplished by changing the time-varying pitch of all four blades exactly in phase. An example of the computed rotor wake evolution is shown in Fig. 8 for an excitation at 12.5 Hz (0.625/rev). It is apparent that in this case the perturbations to the blade pitch inputs manifest as waves of alternating regions of axial expansion and contraction between adjacent groups of tip vortices. The axial contraction of the wake is qualitatively similar to that observed for the impulsively started rotor, with the bundled vortex filaments closely resembling the formation of vortex rings. However, because of the continuous oscillations in the collective blade pitch in this case regions of contraction is followed

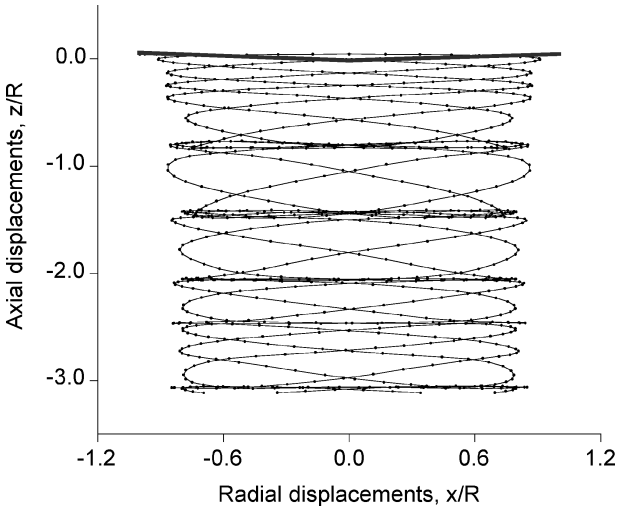

a) $\psi = \psi_b$

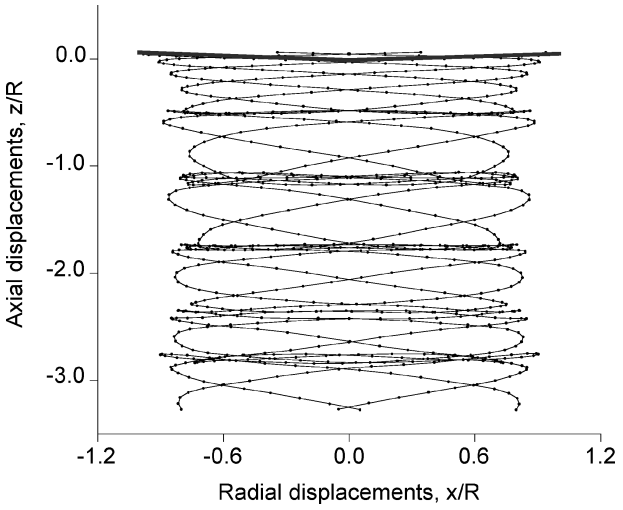

b) $\psi = \psi_b + 380$ **deg**

Fig. 8 Example showing two side views of the rotor wake during an oscillatory collective blade pitch excitation applied at 12.5 Hz (0.625/rev): a) initial time, $\psi_b = \psi$ and b) later time, $\psi_b = \psi + 380$ deg.

by a region of expansion, where the wake vortices have a larger axial separation. This sequence occurs over the whole extent of the wake as the perturbations travel through the wake system at the blade pitch excitation frequency.

The induced inflow at the rotor disk also showed an oscillatory behavior as a result of these periodic waves of contraction and expansion inside the rotor wake. Figure 9 shows the first harmonic measured and predicted amplitude (gain) and corresponding phase of the inflow response across the span of the blade. The inflow values are shown relative to the values obtained in the hovering state. This is different than the presentation given in Ref. 27, but is more intuitive from an aerodynamics perspective. Clearly, the results in Fig. 9 show that the inflow response varies significantly with both the excitation frequency and the radial blade station. For low excitation frequencies, the inflow response is nominally constant over the span. As the excitation frequency increases, however, the unsteady inflow response appears to be concentrated more in the tip region, which is also the trend observed in the experiments. This is an interesting observation because the maximum inflow response corresponds approximately to the spanwise location of the maximum in blade lift.

The results also show that at low excitation frequencies the inflow is much more in phase with the collective pitch excitation (see Fig. 9). As the excitation frequency is increased, however, the phase lag increases quickly over the inboard portion of the blades. This trend observed in the experiments is well modeled by the present free-vortex wake analysis. Ellenrieder and Brinson[27] suggest that the increasing phase lag over the inboard sections of the blade is a result of the trailing vorticity from the blade tips, which, as already mentioned, is the most dominant structure inside a rotor wake. This observation is confirmed by the present analysis.

Cyclic Pitch Excitation

The experiments of Ellenrieder and Brinson[27] also included results for cyclic pitch excitations, although these data were more limited in scope and phase data are not available. In this case, the time-varying pitch of the four blades were excited with a successive phase lag of 90 deg, thereby constituting a cyclic excitation. An example of the wake evolution for a cyclic excitation at 12 Hz (0.6/rev) is shown in Fig. 10. As noted for the case with collective inputs, the wake structure showed a wave-like behavior, with alternate regions of axial contraction and expansion between successive groups of tip vortices. However, because in this case the blade pitch was excited in a cyclic manner these wave structures propagate through the rotor wake in the form of a helicoid.

The first harmonic magnitude of the rotor-induced inflow across the span of the blade to cyclic blade pitch excitation is shown in Fig. 11 for several excitation frequencies. Overall, the predictions showed good agreement with the experimental results. As found for the collective inputs, the inflow response with increasing excitation frequency was more significant near the blade tips. The high inflow amplitude in the region of maximum blade lift was even more pronounced than the corresponding results for the inflow response to collective pitch excitations (see Fig. 9). However, the overall inflow response to cyclic pitch excitation was found to be significantly different from the response to a collective pitch excitation. The diminishing amplitude in the intermediate frequencies below half the rotational frequency is especially interesting because this frequency range determines the basic handling qualities and control characteristics of helicopter.

The results for the radial variation in the corresponding phase of the first harmonic in the predicted inflow response are shown in Fig. 11. No experimental data are available in this case. The phase response was also found to be different from the phase response to collective pitch excitation. Again, however, the phase lag was found to be greater on the inboard parts of the rotor. This is similar to the results obtained for collective pitch excitation, and so it again suggests that the tip vortices are the primary features influencing the evolution of the overall wake.

Wake Dynamics in Maneuvering Flight

The foregoing problems are of much interest and value in understanding the basic effects of pitch control inputs on the dynamics of the wake response. On an actual helicopter, however, significant pilot time-varying control inputs generally only occur during maneuvering flight. Maneuvers comprise combinations of translational and angular motions, including rates and accelerations, and can result in large nonlinear effects on the temporal development of the rotor wake. Pilot control inputs during the maneuver will provide a further source of aerodynamic excitation. Such effects have not been studied sufficiently, and the general features of the wake response under these flight conditions are not well understood.

The effects of a maneuver can be modeled using an additional contribution to the local velocity vector $\boldsymbol{V}(\boldsymbol{r})$ on the right-hand side of Eq. (2) (see Refs. 7 and 18). Angular rates about the roll, pitch, and yaw axes contribute to the wake developments during maneuvers. The equivalent external velocity $\boldsymbol{V}_{\text{ex}}$ resulting from rate-type maneuvers can be determined from a cross product of the maneuver rate vector (p, q, r) and the position vector of a wake element using

$$\begin{aligned}\boldsymbol{V}_{\text{ex}} &= -(p, q, r) \times (x, y, z) \\ &= -(qz - ry)\hat{i} + (pz - rx)\hat{j} + (qx - py)\hat{k} \end{aligned} \tag{9}$$

The first term in Eq. (9), which is the x or streamwise component of the velocity resulting from a pitch rate q and/or a yaw rate r, essentially produces a skewing distortion of the wake. The second

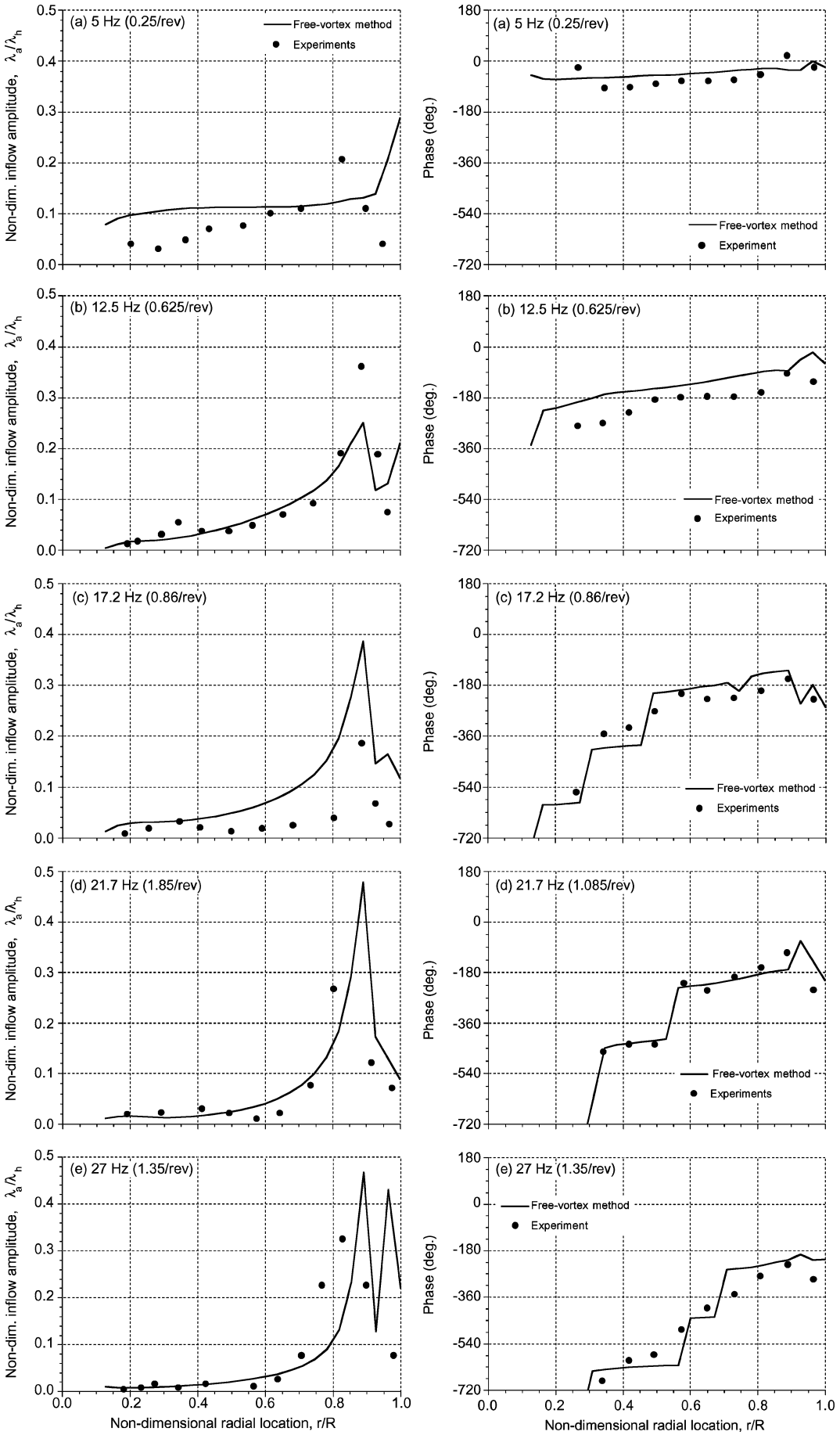

Fig. 9 Radial distribution in the first harmonic of the amplitude (gain) and phase in the unsteady inflow response to harmonic collective blade pitch inputs.

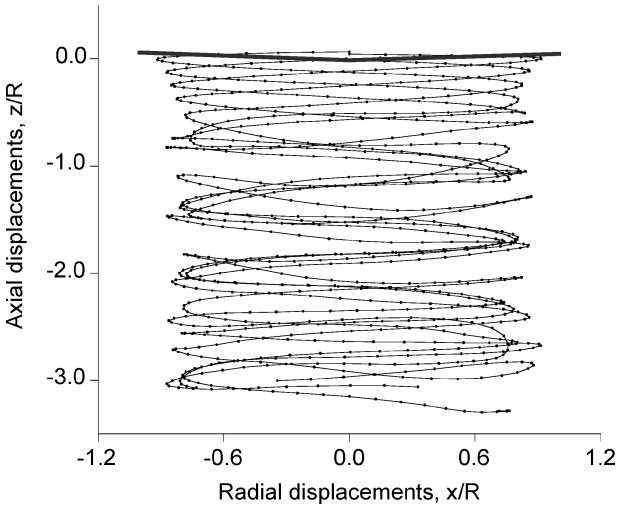

a) $\psi = \psi_b$

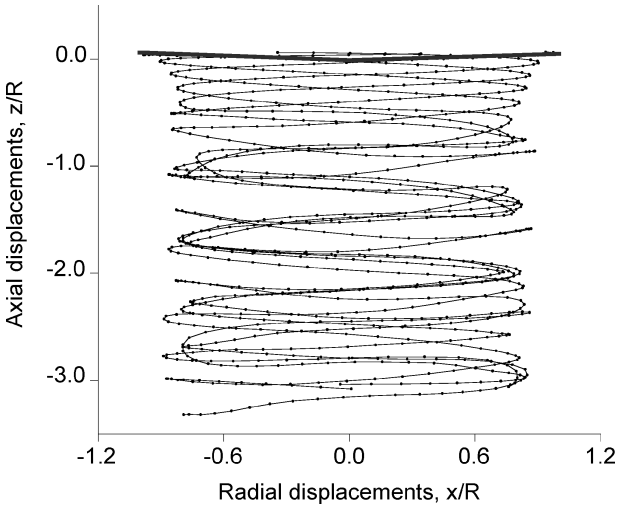

b) $\psi = \psi_b + 380$ **deg**

Fig. 10 Example showing two side views of the rotor wake during oscillatory cyclic blade pitch excitation at 12 Hz (0.6/rev): a) initial time, $\psi_b = \psi$ and b) later time, $\psi_b = \psi + 380$ deg.

term, which is the y or lateral component of the velocity resulting from a roll rate p and/or a yaw rate r, produces wake curvature and also a skewing in the lateral direction. The third $(qx - py)$ term in Eq. (9), results in an asymmetric axial stretching distortion of the wake, which appears like a wake curvature. It has been shown[7,17] that maneuver-induced wake distortions result in significant changes to the rotor-induced velocities and affect the rotor airloads and blade-flapping response.

Pull-Up Maneuver

To explore the wake evolution during simulated piloted flight maneuvers, a series of idealized conditions were examined. Of particular interest was the wake evolution under descending flight conditions, where there is a greater preponderance of blade–vortex and vortex–vortex interactions. Figure 12 shows results during a representative pull-up maneuver from steeply descending flight, such as might be used in some military operations. This simulation was found to contain some of the flow features that have been discussed earlier, including the bundling of wake vorticity.

For these calculations, the rotor was first trimmed to obtain nominally equilibrium conditions at low forward speed ($\mu = 0.04$) and moderately high rate of descent along a 30-deg glide path. The solution was then time marched for a further 20 rotor revolutions to allow any remaining transients to convect out of the solution. The flow conditions subsequently obtained were nominally periodic, but the descent velocity was still sufficiently high to cause some instabilities to develop in the downstream wake behind the rotor. This flight condition formed the initial condition for the subsequent maneuver. Notice that for these conditions, many of the blade tip vortices lie close to or above the plane of the rotor, producing BVIs.

The rapid pull-up was modeled by an increase in collective pitch and longitudinal cyclic inputs to give a disk angle of attack of 15 deg and a nondimensional pitch rate of $q/\Omega = 0.04$. These input conditions were then held, and the wake solution was time marched from the initial condition for a further eight rotor revolutions, at which time the pitch rate was removed, the collective pitch reduced to the starting value, and the disk angle of attack was then maintained at approximately 10 deg using cyclic pitch. The rotor was not trimmed during this process, but the blade flapping was calculated in a time-accurate manner that was consistent with the wake solution.

Notice from the results in Fig. 12 that the temporal wake developments are relatively rapid, with clear evidence that the maneuver initially causes wake vorticity to clump and bundle below the rotor. What is particularly interesting here is that this bundling of vorticity quickly forms into a ring, similar to that shown previously for rapid changes in blade pitch. Notice that this ring of vorticity is convected up toward the rotor and passes through the rear of the disk. As the blades interact with the powerful induced velocity field surrounding this vortex ring, large unsteady airloads are produced (see next). Interestingly, the net effect on the rotor for these flight conditions are symptoms similar to sustained flight operations near or in the so-called "vortex ring state," which is normally obtained only at very high rates of descent.[28,29,‡]

The pitch rate was removed at the end of eight rotor revolutions, and the disk angle of attack was reduced by 5 deg by the application of cyclic pitch. Notice from Fig. 12d that at this point the vortex ring that was first formed has become unstable and has begun to fold over onto itself forming a knot (compare Fig. 4). Figure 12e shows that the upstream loop of the folded ring is then entrained back through the rotor, while the downstream part of the loop is stretched and convects away from the rotor. At about $t + 16$ rotor revolutions, the downstream loop undergoes a further stretching and twisting deformation, which induces a velocity field on the upstream part of the loop that causes it to be convected back up toward the rotor again (see Fig. 12f). This is followed by a further twisting of the vortex loops, so that the loops become more oriented in a lateral direction. Finally, the flow adjustments cause the wake to reestablish a nominally helicoidal structure, and by about $t + 30$ revolutions the wake has returned to a form closely resembling its initial condition.

The rotor thrust variations during this simulated maneuver are shown in Fig. 13. At the beginning of the pull-up maneuver, notice that a transient overshoot of thrust is obtained. This is the Carpenter and Friedovich effect[14] alluded to earlier, where the temporal evolution of the vortex wake results in a delayed buildup of the inflow, and so the thrust is initially larger until these transients have time to die out. Thereafter, the imposed pitch rate (with its effective longitudinal velocity gradient over the rotor disk) causes the wake to be convected up toward the rotor. This produces thrust fluctuations of moderate amplitude as the blades encounters this vorticity. During this time, the vortex ring forms below the rotor, and by about $t + 4$ revolutions the upstream edge of the ring has begun to pass through the rear of the rotor disk.

The high induced downwash effects produced by the ring lead to a progressive reduction in rotor thrust during this process. At about $t + 8$ revolutions, the vortex ring has become unstable and has folded over on itself. Combined with the removal of the pitch rate, this produces another transient thrust overshoot. The vortex ring then passes through the rotor, and thrust fluctuations continue to be produced at a moderate level as the wake vorticity lingers below the rotor plane and the flow subsequently begins to readjust to the new flight conditions. Notice again that these adjustments occur over several rotor revolutions and illustrate the long relative timescales associated with rotor wake developments, in general. Eventually,

‡Data available online at http://www.enae.umd.edu/AGRC/Aero/vring.html.

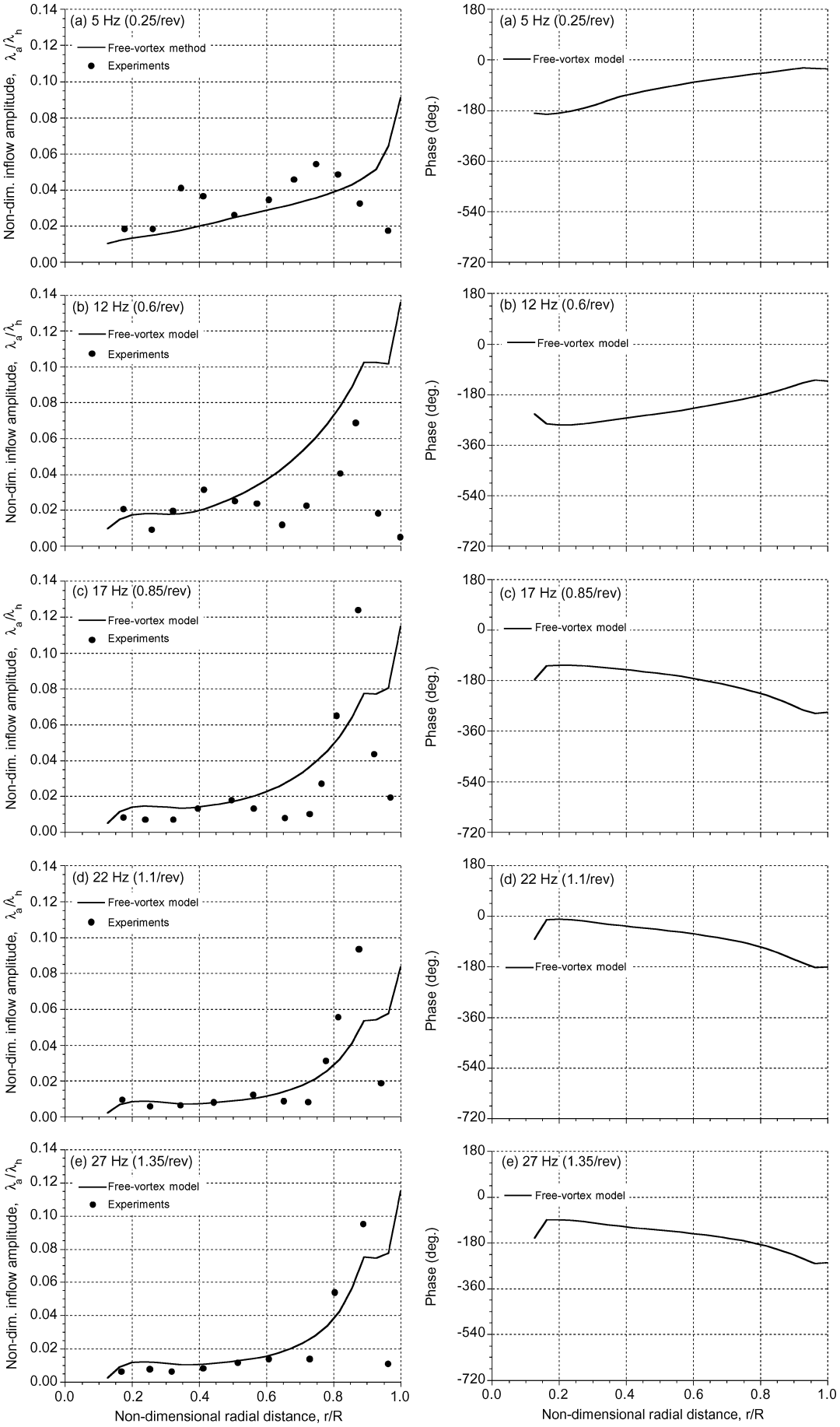

Fig. 11 Radial distribution in the first harmonic of the amplitude (gain) and phase in the unsteady inflow response to harmonic cyclic blade pitch inputs.

the rotor thrust becomes relatively constant as the transient wake adjustments are completed.

Periodic Collective Inputs

A study was conducted to examine the effects of small-amplitude pilot control inputs on the wake evolution and blade loads of a rotor in forward descending flight. The simulation was conducted for a four-bladed rotor following a 6-deg glide path at a rotor advance ratio $\mu = 0.1$. The collective pitch was excited with an amplitude of 1 deg at a relatively low frequency of 0.2/rev. This replicates a precision piloting task along a predetermined glide path, where it is apparent from published results[30] that pilots can introduce small but significant periodic inputs in collective pitch to track the trajectory accurately. The blade pitch inputs also seem to correlate with rotor noise fluctuations.

Figures 14 and 15 shows two sets of snapshots of the top, side, and rear views of the rotor wake. The sets are separated in time by 2.5

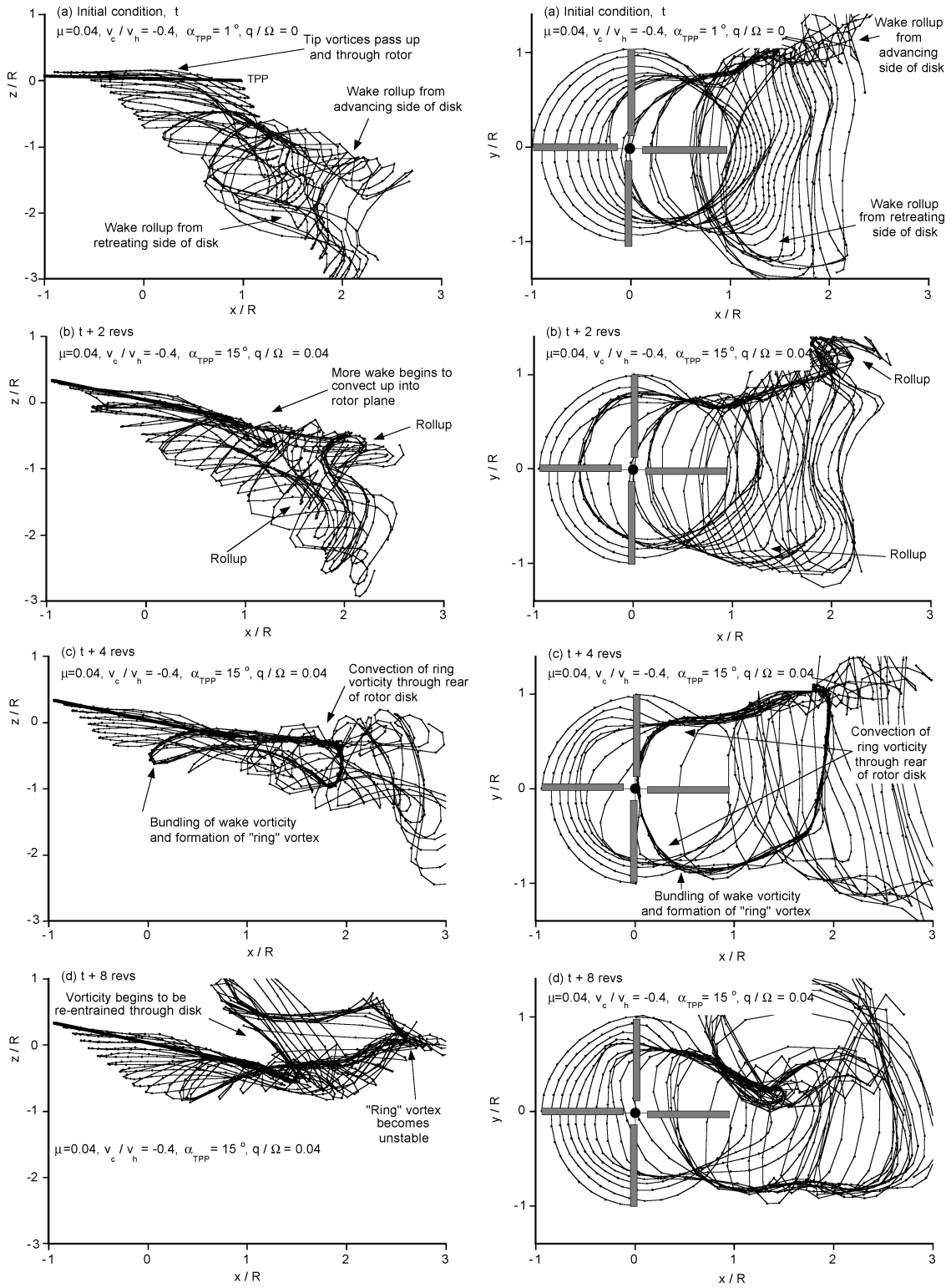

Fig. 12 Snapshots in time of the top and side views of the wake geometry produced on a single rotor during a simulated pitch-up maneuver: a) initial condition, time = *t*, b) *t* + 2 revs, c) *t* + 4 revs, d) *t* + 8 revs, e) *t* + 12 revs, f) *t* + 16 revs, g) *t* + 20 revs, and h) *t* + 24 revs.

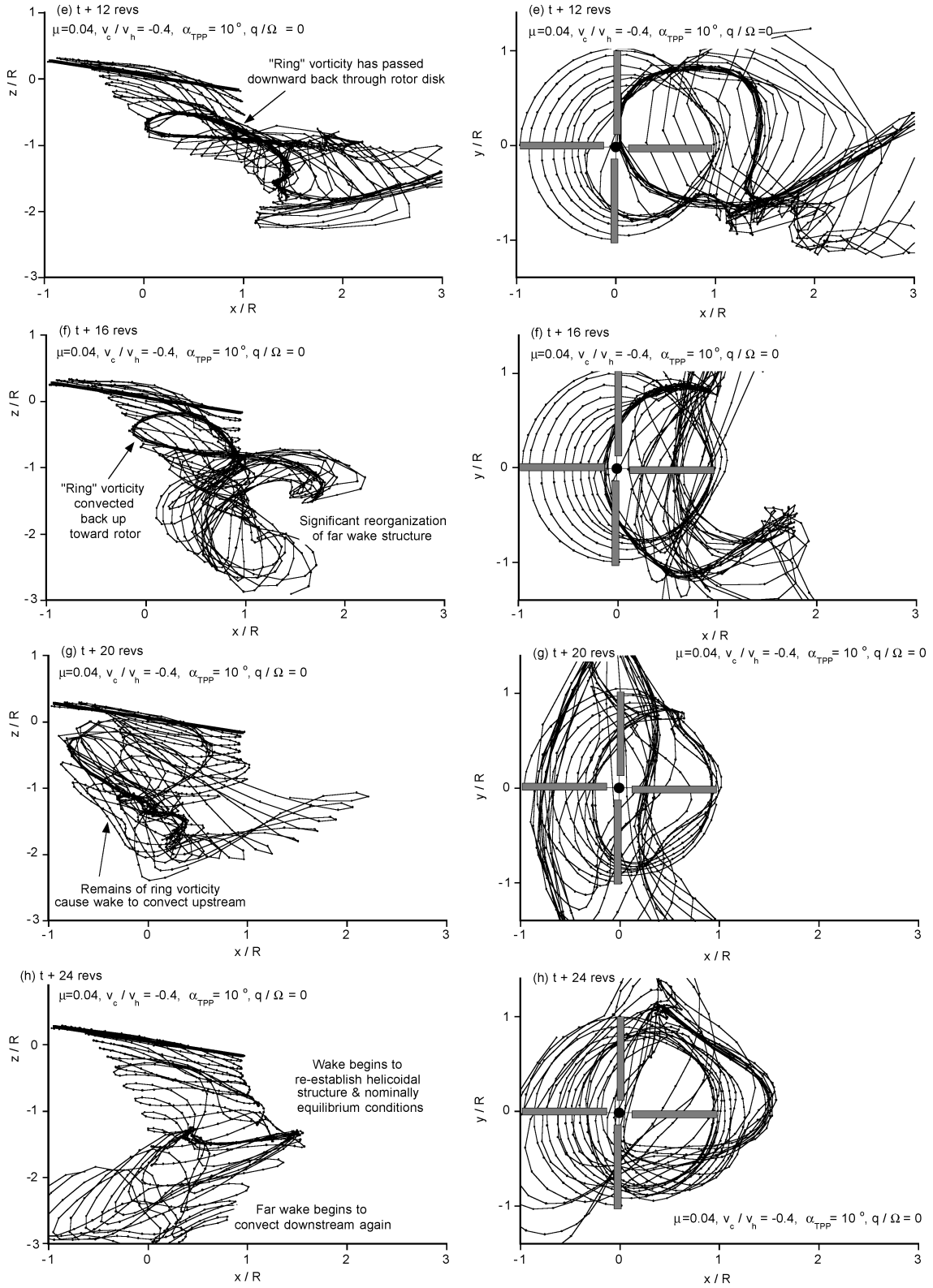

Fig. 12 Snapshots in time of the top and side views of the wake geometry produced on a single rotor during a simulated pitch-up maneuver: a) initial condition, time = *t*, b) *t* + 2 revs, c) *t* + 4 revs, d) *t* + 8 revs, e) *t* + 12 revs, f) *t* + 16 revs, g) *t* + 20 revs, and h) *t* + 24 revs (continued).

rotor revolutions, which represent (approximately) the two extremes in the wake displacements during the collective pitch inputs. In each case the results are compared to the baseline solution, which is for constant collective pitch. For these descending flight conditions, many of the wake filaments lie close to the rotor plane producing BVIs, especially on the advancing side of the rotor disk.

Notice from Figs. 14 and 15 that the effects of small collective pitch inputs are relatively significant and affect both the in-plane and out-of-plane (vertical) wake displacements. In the plane of the rotor, changes in the wake displacements were found to occur mainly in the first and second quadrant of the rotor disk, which is the region that is acoustically important. Many of these locations are potential BVI locations (see next), which is apparent from the side and rear views of the wake.

In particular, notice the changes that take place in the roll up of the tip vortices from the advancing side of the rotor disk. The radial

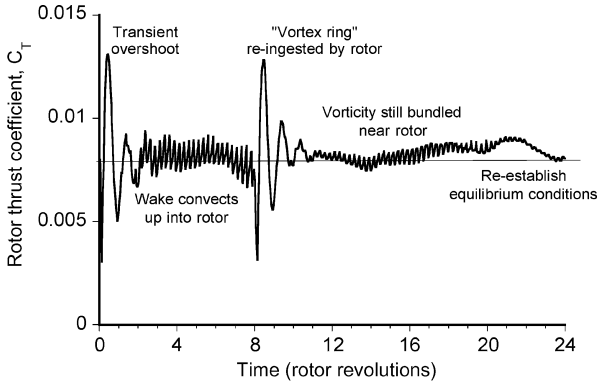

Fig. 13 Time-history of rotor thrust during pitch-up type maneuver.

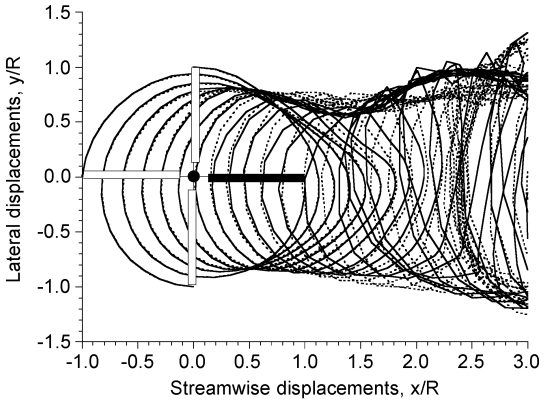

a) Top view, $\psi = \psi_b$

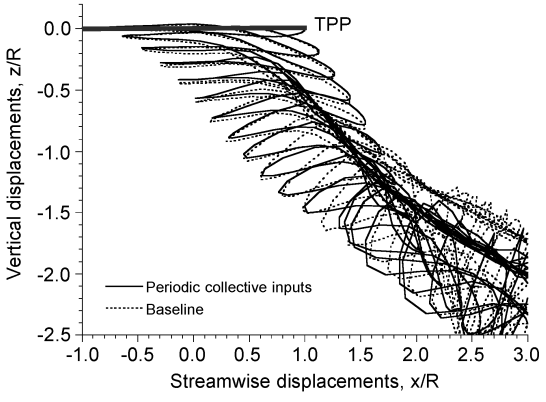

b) Side view, $\psi = \psi_b$

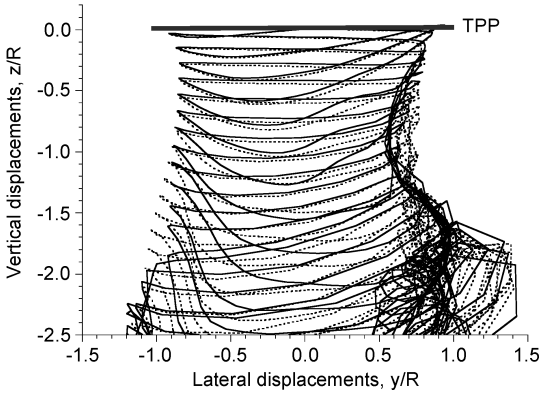

c) Rear view, $\psi = \psi_b$

Fig. 14 Top, side, and rear snapshot views of the wake geometry for a four-bladed rotor in response to low-frequency collective pitch inputs, with time = *t*: a) top view (reference blade is shaded), b) side view, and c) rear view.

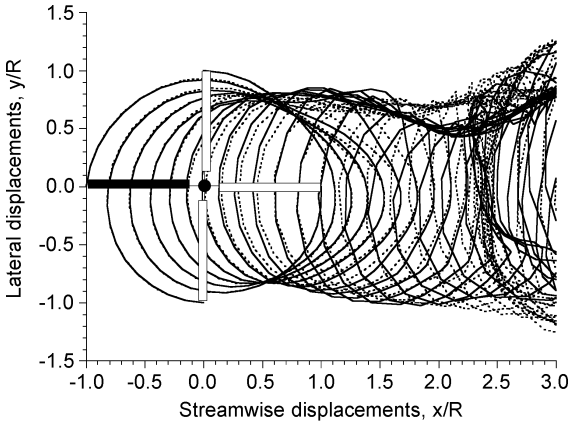

a) Top view, $\psi = \psi_b + 900$ deg

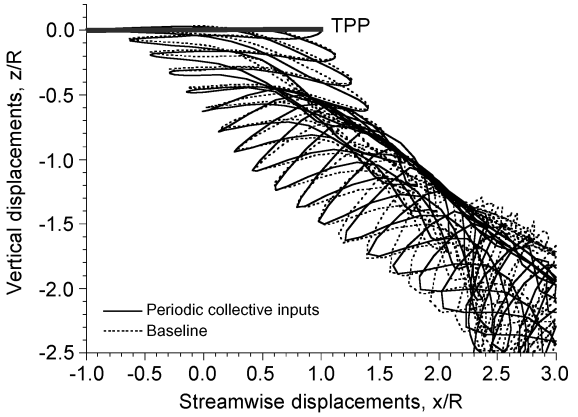

b) Side view, $\psi = \psi_b + 900$ deg

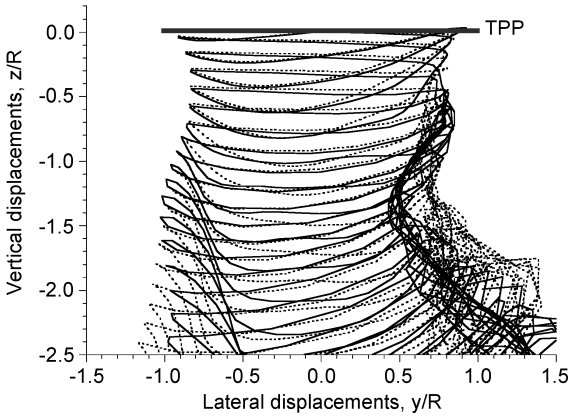

c) Rear view, $\psi = \psi_b + 900$ deg

Fig. 15 Top, side, and rear snapshot views of the wake geometry for a four-bladed rotor in response to low-frequency collective pitch inputs with time = *t* + 2.5 revs: a) top view (reference blade is shaded), b) side view, and c) rear view.

inward and outward movement of the roll up is clearly responsible for the bulk of any changes in the net induced velocity field over the rotor, which subsequently affects the positions of the wake vortices over the rear half of the rotor disk. This again emphasizes the need to model accurately not only the convection of the tip vortices but also the near-field induced effects associated with strain and diffusion so that the close vortex–vortex interactions and overall wake roll-up from the rotor disk can be properly represented.

Figure 16 shows better detail of the tip vortex positions, which is a snapshot of the wake geometry for the reference blade at two instants in time separated by 2.5 rotor revolutions. All of the potential BVI locations are shown for tip vortices that are within either one chord (solid circles) or five chords (open circles) of the rotor disk. With periodic collective pitch inputs, it was found that vertical

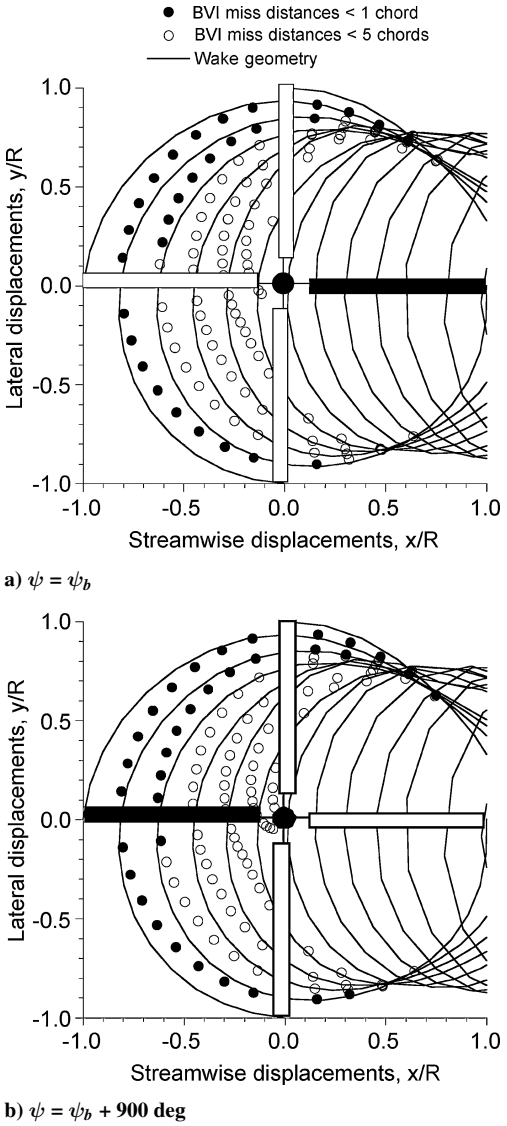

a) $\psi = \psi_b$

b) $\psi = \psi_b + 900$ **deg**

Fig. 16 Top views of the wake geometry and locus of all potential BVI locations for a four-bladed rotor in response to low-frequency collective pitch inputs: a) time $t = 0$ and b) time = $t + 2.5$ revs.

displacements relative to the blades of up to 0.75 chords were produced. These differences will affect significantly both the magnitude and directivity of the acoustics generated by the rotor and demonstrate that the fidelity of the wake modeling will be very important if accurate acoustic predictions are ever to be realized.

Conclusions

This study has used a time-accurate free-vortex method to help understand the transient rotor-wake developments in response to time-dependent blade pitch inputs in both steady and maneuvering flight. The results show how in many cases the wake evolution in response to control inputs is dominated by the bundling of tip vortices and accumulation of vorticity below the rotor, which can then develop into vortex rings. The results obtained were compared to available experimental observations to demonstrate the capability of this class of methods in quantitatively predicting transient rotor airloads and rotor response. The following conclusions have been drawn from the study:

1) A change in rotor operating conditions (through collective or cyclic control inputs) can be accompanied by bundling of individual tip vortices in the wake below the rotor, forming a toroidal ring of accumulated vorticity. This is a behavior also seen experimentally. There is considerable lag in the development of the rotor airloads when these bundles of vorticity are in the vicinity of the rotor.

2) It was found that the starting vortex rings become unstable as they propagate through the rotor wake. The rings tend to develop a series of short wavelength Kelvin waves, which grow in amplitude with time. Eventually, the rings break down as they age or as they are convected further downstream into the far wake of the rotor.

3) Periodic changes in blade pitch control inputs cause the continuous formation and propagation of a series of vortex bundles. In the case of collective pitch inputs, the wake vortices form into a series of stacked rings, whereas for cyclic pitch inputs the bundles take on a distinct helicoidal form. In both cases, the temporal dynamics of the wake evolution has a significant effect on the amplitude and phase of the unsteady flow environment at the blades.

4) Continuous, small-amplitude control adjustments by the pilot appear to be a significant contributor to the temporal evolution of the rotor wake. In maneuvering flight conditions, it was shown how it is possible for the rotor to encounter its own accumulated wake vorticity, in some cases resembling flight in the vortex ring state, which is usually obtained only at very high rates of descent. The extremely complex nature of the wake in these conditions cannot be underestimated.

Acknowledgments

The authors would like to acknowledge Wayne Johnson of NASA Ames Research Center for motivating a more detailed study of this problem and also Robert Ormiston from the U.S. Army at NASA Ames Research Center for his very helpful and insightful discussions about wake evolution and unsteady aerodynamics. The support of Mehandra Bhagwat of U.S. Army at NASA Ames Research Center is also gratefully acknowledged. This work has been supported, in part, by the National Rotorcraft Technology Center under the Rotorcraft Centers of Excellence Program.

References

[1]Leishman, J. G., *Principles of Helicopter Aerodynamics*, Cambridge Univ. Press, New York, 2000, Chap. 1.

[2]Schmitz, F. H., "Rotor Noise," *Aeroacoustics of Flight Vehicles: Theory and Practice*, edited by H. H. Hubbard, Vol. 1, NASA Reference Publication 1258, Washington, DC, Aug. 1991, Chap. 2.

[3]Leishman, J. G., and Bagai, A., "Challenges in Understanding the Vortex Dynamics of Helicopter Rotor Wakes," *AIAA Journal*, Vol. 36, No. 7, 1998, pp. 1130–1140.

[4]Martin, P. B., Pugliese, G., and Leishman, J. G., "High Resolution Trailing Vortex Measurements in the Wake of a Hovering Rotor," *Proceedings of the American Helicopter Society 57th Annual National Forum*, American Helicopter Society, Alexandria, VA, 2001.

[5]Leishman, J. G., Bhagwat, M., and Bagai, A., "Free-Vortex Methods for Helicopter Rotor Wake Analyses," *Journal of Aircraft*, Special Ed. on Rotorcraft Wakes, Vol. 39, No. 5, 2002, pp. 759–775.

[6]Theodore, C., and Celi, R., "Flight Dynamic Simulation of Hingeless Rotor Helicopters Including a Maneuvering Free Wake Model," *Proceedings of the American Helicopter Society 54th Annual National Forum*, American Helicopter Society, Alexandria, VA, 1998.

[7]Bagai, A., Leishman, J. G., and Park, J., "Aerodynamic Analysis of a Helicopter in Steady Maneuvering Flight Using a Free-Vortex Rotor Wake Model," *Journal of the American Helicopter Society*, Vol. 44, No. 2, 1999, pp. 109–120.

[8]Quackenbush, T. R., Keller, J. D., Wachspress, D. A., and Boschitsch, A. H., "Reduced Order Free Wake Modeling for Near Real Time Simulation of Rotorcraft Flight Mechanics," *Proceedings of the American Helicopter Society 55th Annual National Forum*, American Helicopter Society, Alexandria, VA, May 1999.

[9]Barocela, E., Peters, D. A., Krothapalli, K. R., and Prasad, J. V. R., "The Effect of Wake Distortion on Rotor Inflow Gradients and Off-Axis Coupling," AIAA-97-3579, 1997.

[10]Keller, J. D., and Curtiss, H. C., "Modeling the Induced Velocity of a Maneuvering Helicopter," *Proceedings of the American Helicopter Society 52nd Annual National Forum*, American Helicopter Society, Alexandria, VA, 1996.

[11]Rosen, A., and Isser, A., "A New Model of Rotor Dynamics During Pitch and Roll of a Hovering Helicopter," *Journal of the American Helicopter Society*, Vol. 30, No. 3, 1995, pp. 17–28.

[12]Taylor, M. K., "A Balsa-Dust Technique for Air-Flow Visualization and Its Application to Flow Through Model Helicopter Rotors in Static Thrust," NACA TN-2220, Nov. 1950.

[13]Saffman, P. G., *Vortex Dynamics*, Cambridge Univ. Press, Cambridge, England, U.K., 1992.

[14]Carpenter, P. J., and Friedovich, B., "Effect of A Rapid Blade-Pitch Increase on the Thrust and Induced-Velocity Response of a Full-Scale Helicopter Rotor," NACA TN 3044, Nov. 1953.

[15]Jessurun, K. P., Pavel, M. D., and Toet, S., "Apparent Mass Effects on a Stiff-Hinged Rotor Model After Raid Cyclic and/or Collective Inputs—A Flow Visualization Study," *Proceedings of the European Rotorcraft Forum*, Moscow, Sept. 2001.

[16]Tang, L., and Baeder, J. D., "Improved Euler Simulation of Hovering Rotor Tip Vortices with Validation," *Proceedings of the American Helicopter Society 5th Annual Forum*, American Helicopter Society, Alexandria, VA, 1999.

[17]Bhagwat, M. J., and Leishman, J. G., "Time-Accurate Modeling of Rotor Wakes Using a Free-Vortex Wake Method," AIAA-2000-4120, 2000.

[18]Bhagwat, M. J., and Leishman, J. G., "Stability, Consistency and Convergence of Time-Marching Free-Vortex Rotor Wake Algorithms," *Journal of the American Helicopter Society*, Vol. 46, No. 1, 2001, pp. 59–71.

[19]Ananthan, S., Leishman, J. G., and Ramasamy, M., "The Role of Filament Stretching in the Free-Vortex Modeling of Rotor Wakes," *Proceedings of the American Helicopter Society 58th Annual Forum*, American Helicopter Society, Alexandria, VA, 2002.

[20]Bhagwat, M. J., and Leishman, J. G., "Generalized Viscous Vortex Core Models for Application to Free-Vortex Wake and Aeroacoustic Calculations," *Proceedings of the American Helicopter Society 58th Annual Forum*, American Helicopter Society, Alexandria, VA, 2002.

[21]Ramasamy, M., and Leishman, J. G., "The Interdependence of Straining and Viscous Diffusion Effects on Vorticity in Rotor Flow Fields," *Proceedings of the American Helicopter Society 59th Annual Forum*, American Helicopter Society, Alexandria, VA, 2003.

[22]Rossow, V. J., "Convective Merging of Vortex Cores in Lift-Generated Wakes," *Journal of Aircraft*, Vol. 14, No. 3, 1977, pp. 283–290.

[23]Johnson, W., *Helicopter Theory*, Princeton Univ. Press, NJ, 1980, Chap. 9.

[24]Bhagwat, M. J., and Leishman, J. G., "Stability Analysis of Helicopter Rotor Wakes in Axial Flight," *Journal of the American Helicopter Society*, Vol. 45, No. 3, 2000, pp. 165–178.

[25]Ormiston, R. A., and Peters, D. A., "Hingeless Rotor Response with Nonuniform Inflow and Elastic Blade Bending," *Journal of Aircraft*, Vol. 9, No. 10, 1972, pp. 730–736.

[26]Gaonkar, G. H., and Peters, D. A., "Effectiveness of Current Dynamic Inflow Models in Hover and Forward Flight," *Journal of the American Helicopter Society*, Vol. 31, No. 2, 1986, pp. 47–57.

[27]Ellenrieder, T. J., and Brinson, P. R., "The Dynamic Induced Velocity Field of a Model Rotor in Hover Conditions," *The Aeronautical Journal*, Vol. 102, June/July 1998, pp. 331–335.

[28]Drees, J. M., and Hendal, W. P., "The Field of Flow Through a Helicopter Rotor Obtained from Wind Tunnel Smoke Tests," Versl. Nat. Luchtvlab, Rept. A.1205, Feb. 1950; also *Journal of Aircraft Engineering*, Vol. 23, No. 266, April 1951, pp. 107–111.

[29]Leishman, J. G., Bhagwat, M. J., and Ananthan, S, "Predictions of the Vortex Ring State for Single-Rotor and Multi-Rotor Configurations," *Proceedings of the American Helicopter Society 58th Annual Forum*, American Helicopter Society, Alexandria, VA, 2002.

[30]JanakiRam, R. D., and Khan, H., "Prediction and Validation of Helicopter Descent Flyover Noise," *Proceedings of the American Helicopter Society 56th Annual Forum*, American Helicopter Society, Alexandria, VA, 2000.